Polymer 120 (2017) 43–51

Contents lists available at ScienceDirect

Polymer

journal homepage: www.elsevier.com/locate/polymer

Ductility potential of brittle epoxies: Thermomechanical behaviour of plastically-deformed fully-cured composite resins

Mark Turk [a], Ian Hamerton [b], Dmitry S. Ivanov [b, *]

[a] QuEST Global, Unit 12 Brabazon Office Park, Golf Course Lane, Filton, Bristol BS34 7PZ, UK
[b] Department of Aerospace Engineering, University of Bristol, University Walk, Bristol BS8 1TR, UK

ARTICLE INFO

Article history:
Received 8 March 2017
Received in revised form
17 May 2017
Accepted 22 May 2017
Available online 23 May 2017

Keywords:
Composite matrices
Epoxy
Ductility
Brittleness
Thermo-mechanical testing

ABSTRACT

The thermoset matrices that are typically used in structural composites are generally well known for extreme brittleness, sensitivity to defects, and poor performance at complex strain states. These features impede a full material characterisation and an understanding of their behaviour. It is, however, of fundamental importance to separate the scale-dependent and defect-imposed failure from the bulk material performance of epoxies, to enable significant improvements in ductility to be realised. The current paper suggests a new experimental routine for investigating the ductility limits of brittle epoxies and accumulating the large macro-scale volumes of plastically deformed epoxies, necessary to study physical and mechanical properties of cured thermosets following yield. It has been shown that a fully cured, densely cross-linked epoxy can undergo at least 50% of the equivalent plastic strain without loss in stiffness and with no detectable degradation of internal architecture. It has also been shown that the deformed epoxies change their thermo-visco-elastic behaviour. A comparative study of plain and toughened epoxies has shown that the former have higher ductility potential than the systems heavily loaded with thermoplastics. This implies that in order to achieve improvements in thermoset ductility, a revised concept of epoxy modification may be required.

1. Introduction

The major problem associated with the mechanical performance of modern thermoset composites is brittleness which arises, to a large extent, from the behaviour of densely cross-linked polymers. Composites are known to experience the onset of matrix intra-ply cracking, which precedes fibre rupture, and typical values for the strain at the onset of failure are 0.6% for cross-ply laminate composites loaded in tension; 0.2–0.3% for textile composites [1–3]. Early cracking promotes development of critical failure modes such as inter-ply delamination, affects fatigue performance, compromises environmental resistance, and creates serious constraints for some applications such as pressure vessels. Above all, a damaged material will hardly be accepted for quality-critical components. Hence, the premature failure means that the potential of composite materials is far from being realised.

To fight the cracking in thermosets it is crucial to understand (1) the factors accelerating brittle failure and (2) the bulk behaviour of a flawless material. There are serious impediments to the separation of these two phenomena and thermosets are well known for exhibiting extreme sensitivity to the presence of defects [4]. The experiments of Asp et al. [5] have clearly highlighted the reason for this peculiarity, for by testing epoxies in hydrostatic tension they found a dramatic ten-fold drop of strain to failure compared to the values obtained in uniaxial tensile testing. The extreme sensitivity of the material to complex straining causes its intolerance to the presence of any inhomogeneity as it creates a complex stress-strain field around it.

While known for being very brittle, at certain conditions even fully-cured densely-cross-linked thermosets can be tremendously ductile. The largest deformations are seen in experiments undertaken in shear and compression where the thermosets reach characteristic values of 0.3–1.5 of true compressive strain and exceed 0.3–0.8 of shear strain [6–15]. Such ductility has been observed across a range of temperatures, strain rates and polymer systems (the above references include difunctional (diglycidyl ether of bisphenol A), trifunctional (TGAP), and tetrafunctional (TGGDM) epoxies, polyesters, vinyl esters, polystyrene, and polycarbonate resins). A characteristic ductility was also observed in

* Corresponding author.
E-mail address: dmitry.ivanov@bristol.ac.uk (D.S. Ivanov).

http://dx.doi.org/10.1016/j.polymer.2017.05.052

bending response of cured epoxies [16,17]. The plastic flow has a characteristic pattern for many polymers: in general, they tend to show softening soon after the onset of yielding, then a large plastic plateau, before hardening prior to failure. It should be noted though that the shape of stress-strain curve may be strongly influenced by sample-press constraints [6,15], history of deformation [10], and sample shape [14]. At the hardening stage, the polymers may reach characteristic stress values of the order of 200 MPa, thus absorbing significant energy through deformation history.

The shear stress curves are similar, but normally do not exhibit the characteristic hardening stage. Even though this is much harder to achieve in practice, the high yielding of thermosets can be observed in tension as well. Odom and Adams [4] observed strong scale effect in toughness and tensile strength when testing epoxy samples. Hobbiebrunken et al. [18] produced fine epoxy fibres and tested them in uniaxial tension. Refining the fibre diameter helped to minimise the testing volume and hence, reducing the probability of obtaining a defect within. This precaution made possible the achievement of high plastic deformations for these fibres and even necking, while reaching a tensile strength of 166 MPa (for the HexFlow®RTM6 resin system). A similar concept of testing thin fibre-type samples was then utilised in the study of Misumi et al. [19] who also found exceptional ductility and energy absorption of micro samples.

Thus, while sensitivity to defects is determined by the type of loading, it can be suggested that the bulk material has high potential for plastic flow at various loadings. However, the premature brittle failure often does not allow a material's behaviour to be studied beyond the point at which sample disintegration occurs. This defect-induced failure should not be regarded as the material's strength, but instead it should be treated as a function of sample constraints, manufacturing methods, and quality of surface finish. Along with the study of these failure features, it is equally important to investigate the actual material response and, most importantly, the mechanisms driving these deformations.

The physical mechanisms behind softening, flow, and hardening are disputable. The softening may be related to volume relaxation occurring in the glassy state [10], however some experiments show volume reduction upon yielding onset [20]. The plastic flow at constant load level may be related to transition from the glassy to the rubbery state, where main chain reorientation becomes possible in the polymer. Mechanisms of epoxy flow can be related to the properties of the deformed polymer and need to be studied further.

This level of ductility and toughness observed in matrices is hardly seen in composites even when loaded perpendicular to fibres. The most important reason to account for this is multiaxial straining which matrices experience at the micro level. A high Poisson's contraction of the matrix is not allowed by stiff fibres. The constraints in the fibre direction create transverse and longitudinal stretching of the matrix even when the composite is exposed to pure transverse tension. Additionally, the stiff fibres act as stress concentrators and the interfaces promote failure initiation sites. On the other hand, shear-induced plasticity in epoxies is also well known from testing off-axis ±45° laminates, where unidirectional plies at the meso-level (and consequently the matrix at micro-scale level) are subjected to a combination of shear accompanied by longitudinal tension and slight transverse compression. Summarising these observations, it becomes evident that thermosets are intolerant to multi-axial strain states (typically values of around 0.6% volumetric strain are critical), moderately ductile in uniaxial tension (4–6% is commonly observed strain to failure), and extremely ductile in pure shear (with 40% shear angle to be expected).

The current paper suggests a new experimental programme aimed at understanding deformability of epoxies beyond their current limits imposed by composite architecture, thermal properties of fibres, and manufacturing methods. In the long run, this inform novel composite development strategies and define theoretical limits of composite behaviour. The specific aims are: (1) to explore the bulk material behaviour up to the limits of its performance; (2) to test stiffness degradation and the evolution of physical properties of plastically deformed epoxies (in addition to the previously reported effect such as yield stress evolution, softening behaviour change [10], and aging [21] resulting from plastic cycling); (3) to compare various grades of epoxies and study the implication of toughening on the ductility of as-manufactured and plastically deformed materials.

Two epoxies commonly used in aerospace and automotive industry have been selected for this study:

a) A difunctional epoxy intended for resin transfer moulding: displaying low viscosity, low exotherm, low curing temperature, transparent following cure, designed for efficient manufacture of large components. This resin will be referred as liquid moulding (LM) resin;
b) An epoxy blend used in prepregs for in-autoclave manufacturing: highly toughened with thermoplastic particles, very viscous, opaque following cure, designed for high energy impacts, hereafter referred to as autoclave toughened (AT) resin.

The characteristic properties of these resins are given in Table 1. The particular choice of these resins was dictated by the intention to probe the new experimental programme for most different materials and assess the implications of toughening on the ductility of these resin system.

The paper explores the behaviour of these resins in compression and studies the thermal (DSC), mechanical (shear loading) and thermo-mechanical (relaxation under thermal cycling) behaviour of the fully-cured and plastically-deformed samples.

2. Sample manufacturing

Manufacturing of AT samples followed the routine prescribed for composite prepreg manufacturing. Sheets of epoxy (10 plies of 0.6 mm thickness each) were laid on an aluminium tool, surrounded by the cork barriers to prevent leakage under pressure applied during curing, debulked, and then consolidated and cured in autoclave at 180 °C and 7 bars pressure.

LM samples were mixed with the extra-slow hardener in ratios as specified by the relevant data sheets, poured into a silicone mould, and degassed in vacuum at room temperature. No boiling could be seen at the end of degassing. The resin was then cured for 7.5 h at 65 °C as specified by the manufacturer's data sheets. The DSC analysis (discussed later) demonstrated that the resin had been completely cured (less than 1% of residual exotherm heat flow compared to the total heat generated by the complete cure of the resin).

The samples were then polished to eliminate surface porosity and defects using sand paper of grades 120, 800, and then 2500 sequentially. The cured samples of the non-toughened epoxy are transparent with no visible through-thickness or surface defects apart from the rare residuals of polished-off surface pores.

3. Experimental programme

3.1. Flat compaction testing

Being armed with an understanding that any tensile straining

Table 1
Basic material properties given in available data sheets.

	LM epoxy	AT epoxy
Cured density, g/cm^3	1.10–1.15	1.20–1.30
Recommended curing temperature, °C	50–65	180
Glass transition temperature, °C	80–90	190–200
Young's modulus, GPa	3.0–3.5 (Tensile modulus)	3.0–3.5 (Flexural modulus)
Stress at failure, MPa	69–75 (Tensile strength)	140–150 (Flexural yield strength)
Strain to failure, %	3–4 (Tensile test)	4–5% (Elongation at yield)

may accelerate premature failure, the compression test has been selected as a primary instrument to force yielding in the epoxy. The flat compaction is particularly attractive as it does not involve clamping and does not create unnecessary stress inhomogeneity. The major challenge about this test is to achieve low friction between the tool plates and the samples so that the epoxy are allowed to expand. Without the flow, the constrained sample becomes subject to pure hydrostatic compression and can exhibit hardly any levels of plasticity. The low friction has been achieved by introducing a layer of clay wrapped in polyamide release film. The film-clay sandwiches were placed between the top and bottom surfaces of the sample, which provided sufficiently free sliding. The estimation of the friction coefficient has been achieved by comparing transverse flow in different directions (discussed below in the results section) and it has been concluded that this does not exceed a value of 0.005 throughout the test. The friction adds low compressive stresses along the width and length of the sample providing a comfortable (from the viewpoint of delaying failure) triaxial compression state. The compression test has been realised using an Instron Universal Test apparatus with a 600 kN load cell and rotating upper platform self-adjusting to the direction of load.

The compaction test has been targeted at identifying the relation between applied stress and plastic through-thickness, in-plane, and equivalent strains. Thus the strain measurements have been carried out after the test but not *in-situ*. The samples have been slowly loaded to a predefined stress level (0.5 mm/min), unloaded at the same speed (it has been found that fast unloading may result in cracking upon load removal), photographed, examined for through-thickness deformation, and compacted to a higher load level. Both the epoxies appear to be intolerant to repetitive loading and at the advanced deformation stage samples rarely survived more than three loading-unloading cycles to reach the same load level as the samples loaded only once. While strongly impacting failure behaviour, repetitive loading did not affect the shape of stress-strain curves. Each point in the diagrams discussed below (Fig. 1 and Fig. 2) corresponds to a sample brought to a particular load level and unloaded without sample disintegration. Every sample provides either one (in most cases) or several points. More than 14 samples constituted the data for compaction diagrams for each of the epoxies.

The initial in-plane dimensions of rectangular samples agree with the dimensions required for the standardized Iosipescu shear test: 71 by 20 mm^2. This shape allows cutting the notched samples for shear testing from the pre-deformed compaction samples and hence, studying the properties of the deformed epoxies. The original thickness varied in the range of 3.6–3.9 mm for LM samples, and AT was available in two batches of 3.3–3.5 and 2.3–2.6 mm. The dimensions of the deformed shape have been evaluated through both the image analysis and direct measurements of in-plane and through-thickness dimensions. The measurements of in-plane elongations and through thickness contraction have been performed for corners and central point along the sample sides. For a limited number of samples (not shown on the graphs mentioned above), the volume change associated with the deformations has been measured by immersing samples in water.

3.2. Shear testing

Shear responses have been tested utilising the standardized double-V-notched Iosipescu test [22], but digital image correlation (DIC) was used to measure deformation rather than strain gauges (which were recommended in the standard). As confirmed by the DIC, the zone between notches is subjected strain state approaching pure shear. The effective strain is taken as an average over the

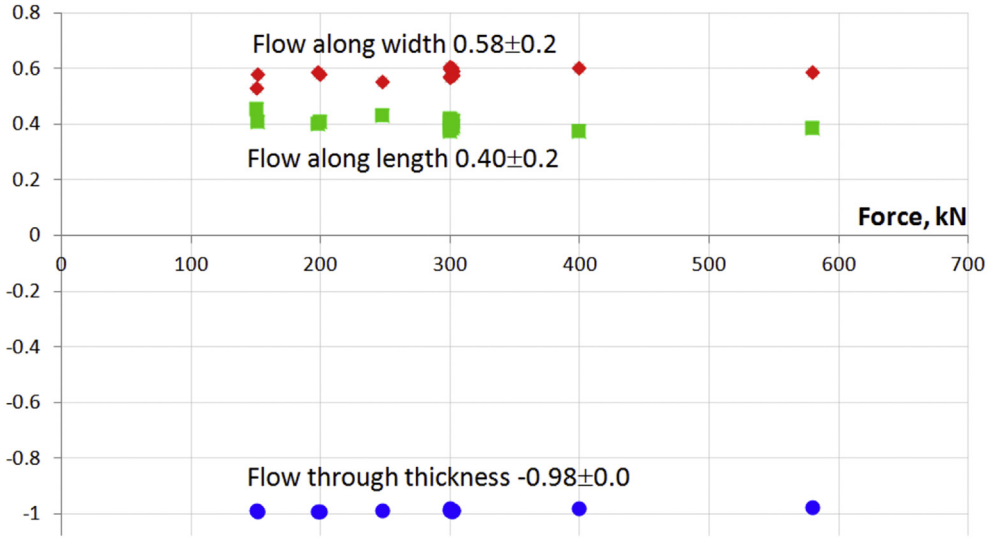

Fig. 1. Flow directions n_i shown as function of applied load for LM samples.

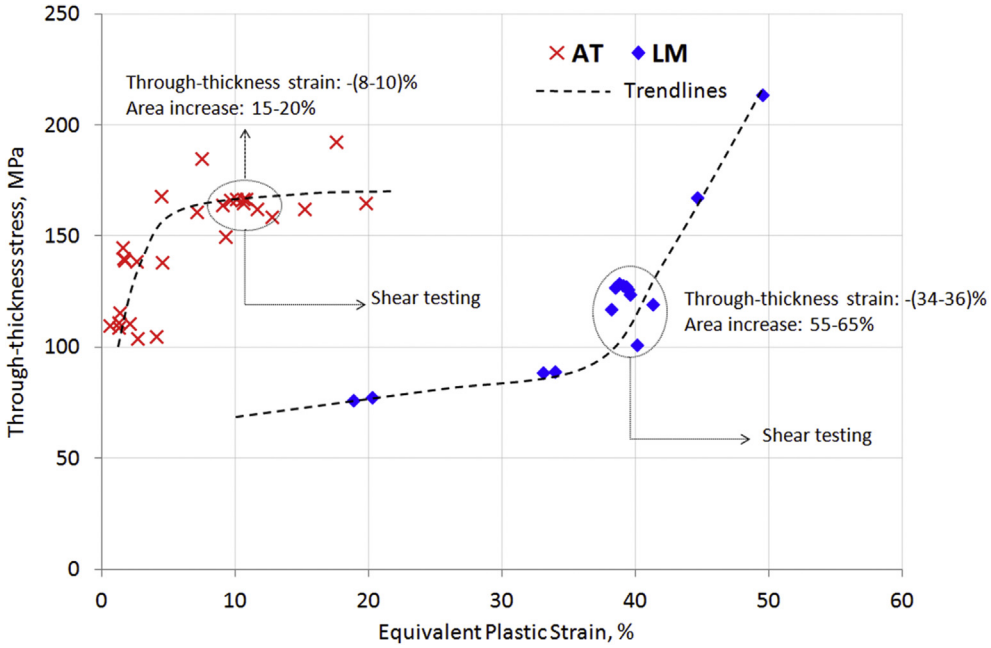

Fig. 2. Stress in through-thickness direction (applied force normalised by the actual area of plastically expanded specimen) *versus* equivalent plastic strains in flat compaction test for two epoxy systems.

narrow zone connecting the notches (Fig. 4). The zone width roughly corresponds to the notch radius (1.3 mm). The effective shear stress acting in this zone is well approximated by the applied force normalised to the cross-section area (the product of thickness and distance between the notches). Six samples of both LM and AT epoxies were tested for each configuration of non-compacted and pre-deformed. The samples were painted in white and covered with black speckle pattern using acrylic spray paints. Commercially available DIC software has been utilised for 2D single camera measurements. Homogeneous monochrome illumination has been used during testing. The camera covered the surface area of most of the sample with the zone of interest placed in the centre, the facet size (a rectangular area where displacement is matched, sometimes referred as 'subset') has been taken sufficiently large to provide stable measurements and eliminate the noise: 17 pixels, which corresponds to the linear size of the area ~0.6 mm. The step size has been chosen as 12 pixels. The shear strain between the notches was taken as strain averaged over rectangular area spanning from one notch to another and spreading 1.3 mm in width (the notch fillet radius).

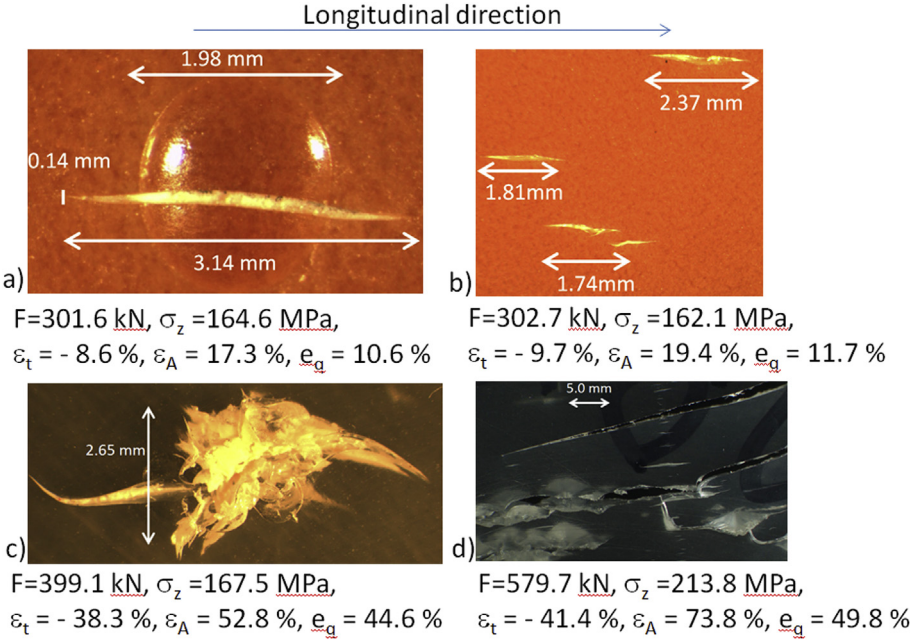

Fig. 3. Typical cracks observed in the material prior to sample disintegration: (a–b) AT (toughened), (c–d) LM. The denotations: F – applied force, σ_z – actual stress in through-thickness direction (normalised to the deformed area), ε_t - relative contraction of sample in thickness direction, ε_A - relative increase of sample area, ε_q- equivalent plastic strain.

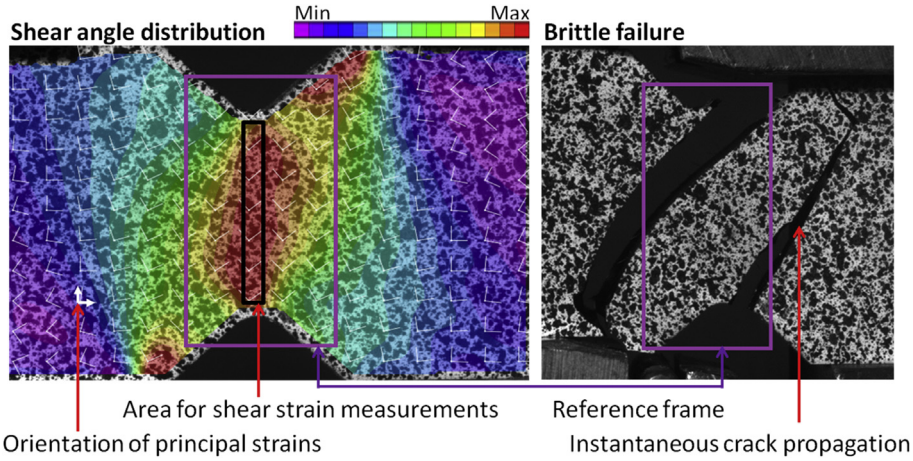

Fig. 4. Typical shear strain distribution in the Iosipescu test and the typical brittle failure (Please see colour version of the Figure in the online version of the paper).

To test plastically deformed samples the thickness, the non-deformed samples were polished to the thickness of the compacted samples to avoid the size effects of epoxies.

3.3. Thermal analysis and thermomechanical testing

Differential scanning calorimetry (DSC) was performed on uncured samples in hermetically sealed aluminium pans at a fixed rate of 10 K/min under nitrogen (40 ml/min). Cast (non-deformed) and pre-deformed samples 12.1–13.6 mg were polished down to 1 mm in thickness prior to placing them in the pans.

The relaxation behaviour of pre-deformed and non-deformed samples was explored using compression loading during thermal cycling. The load was applied by means of heat plates installed on the Instron with 100 kN load cells. All the samples were polished prior to testing: pre-deformed samples down to 2.5 mm thickness, and cast (non-deformed) samples down to 3.9 mm. The samples were pre-loaded, then the position of the loading plates was fixed and material response upon thermal cycling was recorded.

4. Compaction tests

The non-equality of in-plane dimensions results in different expansion along the sample length and width. For the LM epoxy the engineering plastic strain along the length constituted roughly 56% of the through-thickness strain and the plastic strain along the width was about 77% of the total. For AT the ratios were similar: 62% and 77% correspondingly (all the given values obtained using linear regression of engineering strains). The plastic flow directions, n_i, calculated as the ratio of strain deviator to equivalent plastic strain, show that the deformation pattern remains practically independent of applied load for LM – Fig. 1.

$$n_i = \frac{\varepsilon_i^p - \frac{1}{3}\left(\varepsilon_x^p + \varepsilon_y^p + \varepsilon_z^p\right)}{\sqrt{\frac{2}{3}\left(\varepsilon_x^{p^2} + \varepsilon_y^{p^2} + \varepsilon_z^{p^2}\right)}} \quad i = x, y, z \tag{1}$$

where ε_i^p- are plastically accumulated (engineering) strains along the length (x), width (y) and thickness (z) directions. Strictly speaking these deformation characteristics are only applicable for small deformations. However, to a first approximation it gives a good indication of flow peculiarities and a homogeneous spreading with no switch in deformation modes was observed. This could be due to the pronounced change in friction coefficient or development of damage-induced anisotropy. The flow in AT specimens is somewhat different. The flow measurements show a high scatter and unclear trend beyond 250 kN. Above this load level the flow measurements become stabilized. Seven samples loaded up to 300 kN showed practically the same pattern as Prime 20: along the length 0.38 ± 0.03, along the width 0.58 ± 0.03, and through thickness −0.97 ± 0.01.

The relation between through-thickness stress and equivalent plastic strain is summarized in Fig. 2. Loading above the maximum stress/strain is hard to achieve without breaking the samples. The maximum achievable strain is identified as 20% equivalent plastic strains for AT and 50% for LM.

The failure mechanisms appear to be different in these epoxies. In both the cases cracking is not an instantaneous failure event as would be commonly expected for epoxies. Considerable numbers of cracks gradually develop and propagate in a stable fashion (Fig. 3). In AT, Fig. 3 a–b, failure is preceded by the formation of small cracks propagating predominantly in parallel to the long sides of samples (even though the small fluctuations of crack directions are noticeable). The disintegrating cracks tend to deviate from the longitudinal direction, sometimes gradually turning to 90°, when approaching sample corners. The failure surfaces look mostly smooth and “clean” as if this was a brittle failure except for a few step-wise deviations from the general trend line. The cracking does not necessarily match the locations of visible defects, but pores clearly promote the crack onset. LM, Fig. 3 c–d, exhibits a more complex failure pattern. Along with the quasi-brittle cracking the epoxy tends to develop “smashed” zones where individual failure events can hardly be distinguished. The presence of these crazing regions allows stating that LM can and does fail in a non-brittle fashion. The crack initiation is seen at and above 40% equivalent plastic strain for LM and 10% for AT (*N.B.*, these values should not be interpreted as the failure criteria, they are indicative for this particular test only). The samples intended for the post-compaction shear testing were preloaded up to these strain levels.

Both the epoxies demonstrated the potential for extremely ductile behaviour, which can hardly be observed in any other type of testing. Against expectations, under idealised conditions the toughened system appears to be less ductile than the so-called brittle plain epoxy. It yields at a higher stress levels but cracks generated during the deformation develop in brittle fashion and do not allow for achieving more than half of the plastic strains exhibited by the plain system. The latter goes through enormous deformations and achieves exceptionally high stress level (above 200 MPa) prior to non-brittle failure. It can be suggested that the micro-scale inhomogeneity and presence of epoxy-toughener

interfacial regions create local stress concentration and promotes rupture. Hence, potentially the plain epoxy can accumulate much higher energy during failure. It should be emphasized though, that in practice the picture is the opposite. Any presence of deformation inhomogeneity along with tensile straining results in premature failure of both the epoxies. The toughened system though is capable of reaching higher stress levels at failure and hence, exhibits a better resistance to applied loading.

5. Mechanical and physical behaviour of deformed epoxies

5.1. Shear tests

Shear testing is used to understand how induced plasticity affects the properties of the epoxy matrices. The materials are known for the high cross-link density of covalent bonds in the formation a large inter-connected network. Hence, it could be anticipated that large deformations damage the molecular architecture. The first indicator of this damage is stiffness degradation. It is also important to measure the evolution of stress-strain response.

The DIC provides information on all the strain components across the entire area of interest. It clearly shows that for all the samples and for both the epoxies failure is brittle, *i.e.* instantaneous rupture following the planes perpendicular to the action of first principal strain (Fig. 4). The brittle failure occurs irrespective of the number of accumulated plastic deformations and the epoxy type. This agrees with the known observations for torsion and tensile high-yield testing of epoxies [8,18].

Stiffness has been measured as the regression of the stress-strain curve taken between 0.2 and 0.8% of measured shear strain. The maximum strain levels are chosen to be higher than specified by the standard in order to represent effective behaviour during the linear deformation stage rather than an instantaneous modulus in the very beginning of the curve. We believe it gives a better idea of the effective changes in the epoxies during the deformation along with eliminating scatter associated with the uncertain initial stage of deformation. The results, shown in Table 2, indicate that practically no change in stiffness of AT and a 9% drop in stiffness for LM are observed along with the increase in experimental scatter. These measurements show that large deformations are not detrimental for the epoxy stiffness, although LM may exhibit a small reduction in shear modulus at ~40% of equivalent plastic strain.

Table 2
Shear moduli of deformed and undeformed base-line epoxies.

	LM	AT
Shear modulus of base-line epoxy, GPA	1.01 ± 0.08	1.09 ± 0.08
Shear modulus of pre-deformed epoxy, GPA	0.92 ± 0.24	1.12 ± 0.15

The shear diagrams, shown on Fig. 5, are in good correspondence with the compression tests. LM exhibits substantially higher deformation at failure than AT, whereas AT reaches higher stress levels at the beginning of the deformation. The strain to failure of AT does not evolve substantially whereas there is pronounced drop for LM. The shape of the diagram remains similar except for a disappearance of the local softening on the LM curve between 2 and 10% of shear strain.

5.2. Thermal analysis of LM epoxy

Differential scanning calorimetry (DSC) has been used to develop an insight into the internal architecture of the deformed polymers. From this point onwards only the LM epoxy will be discussed. Prior to the investigation of complex heterogeneous systems, it is primarily important to understand the physical processes occurring directly in the pure epoxy.

Heat flow profiles for the deformed and non-deformed epoxies are dissimilar - Fig. 6. The non-deformed epoxy exhibits a known pattern: additional energy is required to exceed the glass transition temperature (83 °C) followed by a small exotherm indicating that residual curing is taking place; the data suggests that the epoxy has undergone almost full cure as the exotherm between 95 and 130 °C constitutes not more than 1% of the total energy at curing of LM. The deformed material displays a peak at 70 °C with obvious local instabilities in the curve. Then, at the glass transition the material demands substantially lower heat than the base-line material. Eventually, two curves converge at 120 °C before diverging again at 155 °C. As the material is effectively fully cured, the energy release at 70 °C can hardly indicate an additional curing. Apparently, this is

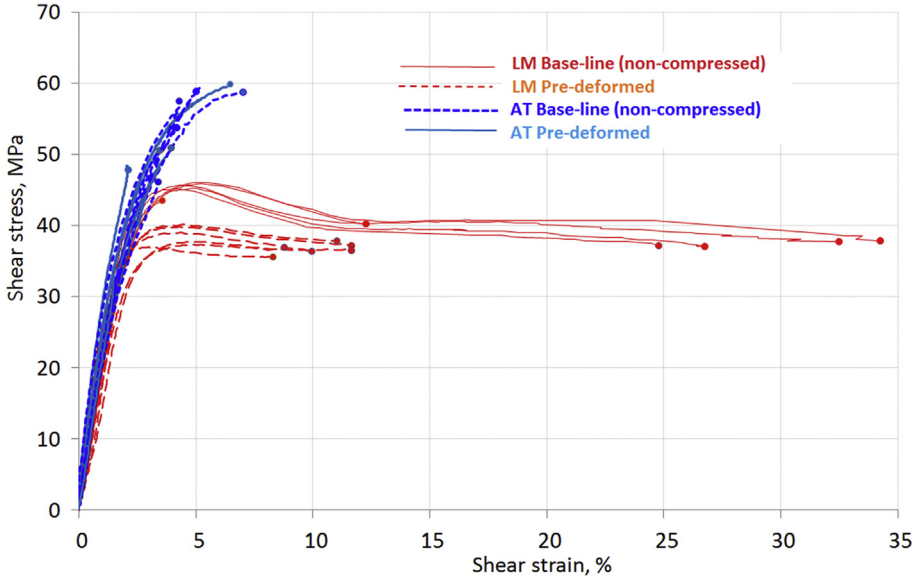

Fig. 5. Shear stress-strain curves obtained from Iosipescu shear test (NB: x-axis is shear strain = 0.5 shear angle). Circles denote the moment of failure.

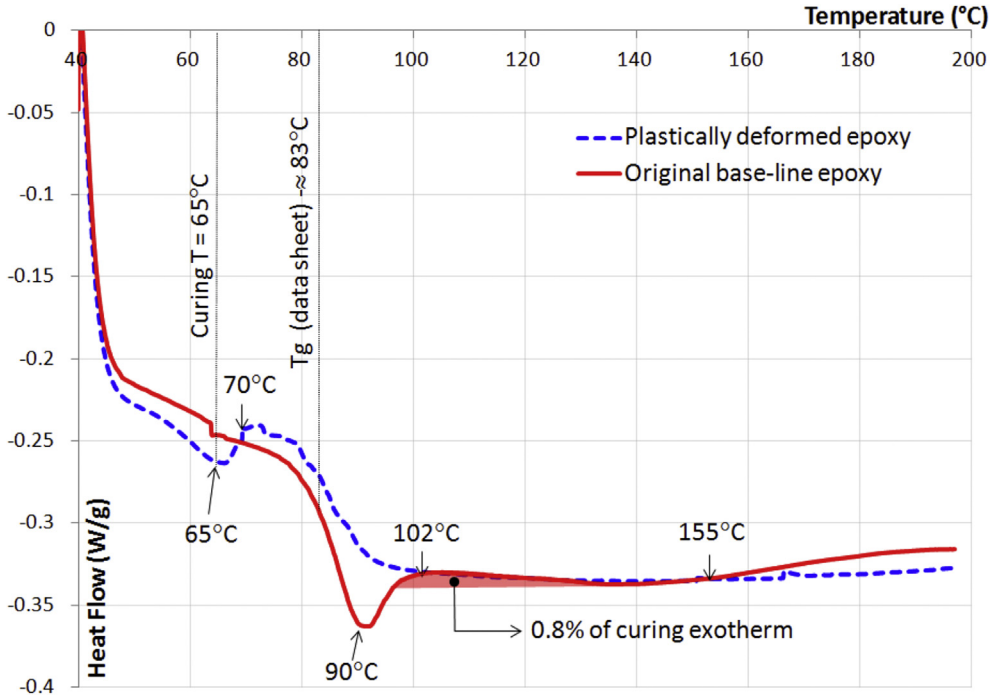

Fig. 6. Heat flow profiles for deformed and non-deformed LM resin.

an indication of accumulated energy which has been released at this temperature in the form of heat.

5.3. Relaxation behaviour of pre-deformed and original samples

To validate the assumption that energy of pre-deformed samples can be released in the form of heat, a thermal cycling of samples at a fixed applied load has been conducted. The idea of the test is to heat and cool a stressed material while recording the stress which it generates. It was anticipated that the accumulated energy of pre-deformation must exhibit itself in the *increase* of stress when heating.

The plastically deformed and pristine epoxy samples were first loaded in compression with heat plates mounted on Instron to 15–16 MPa (elastic deformation range). At this load level the displacement has been fixed. Temperature has been raised in 10 °K steps (each ramp was completed in roughly 3 min). Every temperature ramp has been followed by approximately 5 min dwell allowing the material to be fully heated. The dwell was also needed to accommodate the stress relaxation and get the force reading stabilized. The pristine epoxy has exhibited small relaxation beyond 70 °C and dramatic stress drop at glass transition temperature – Fig. 7. The stress has not been restored upon cooling. In fact the opposite was shown and stress continued decaying until the sample and heating plates were disengaged at 60 °C.

The pre-deformed sample shows completely different behaviour. After each temperature ramp the reaction stress first ***increased*** before relaxing as the lower load level. This confirms the assumption that the energy accumulated during first stage of compaction was then released upon heating. This energy though is insufficient to result in an elastic spring back behaviour at room temperature. The spikes in stress response continued until reaching the glass transition temperature. The stress relaxation beyond the glass transition has been pronouncedly stronger in the original epoxy configuration. However, the stress drop at glass transition temperature is many times lower. Similar to the base-line system, the stress continued decreasing upon cooling. Nevertheless, upon reaching room temperature the sample still withstood 43% of the initial load level.

In agreement with widely recognised observations of shape memory, the pre-deformed samples of both the resin systems fully recovered its shape when thermally cycled above the glass transition temperature. However, when the thermal cycling was conducted at the compression load the shape of both pre-deformed (as well as pristine) samples practically did not change.

6. Results and discussion

The experimental programme was arranged in a way to assess the physical transformations occurring with compacted samples to explore the potential for ductility. The yielded, fully cured, pre-deformed samples were tested both mechanically and thermally. The chain of tests, conducted in this study, demonstrated several peculiarities in the behaviour of the epoxy. The key observations are highlighted below:

1. In agreement to a previously reported experiments on the deformation of cured epoxies, the samples subjected to compression revealed a high level of plastic deformations both for toughened and non-toughened resin systems. The toughened system exhibited a significantly higher level of yield stress, but a compromised performance in terms of strain to failure. Yield stress *versus* strain-to-failure difference was observed both in compression and shear loadings. This gives an indication that the particles of thermoplastic toughener may act as stress concentrators and create complex multi-axial straining in their vicinity affecting the resin ductility.
2. Both the toughened and non-toughened samples retained their stiffness despite the large plastic deformation achieved in compression. This may indicate that the cross-link architecture was not damaged. A full recovery of sample shape upon thermal

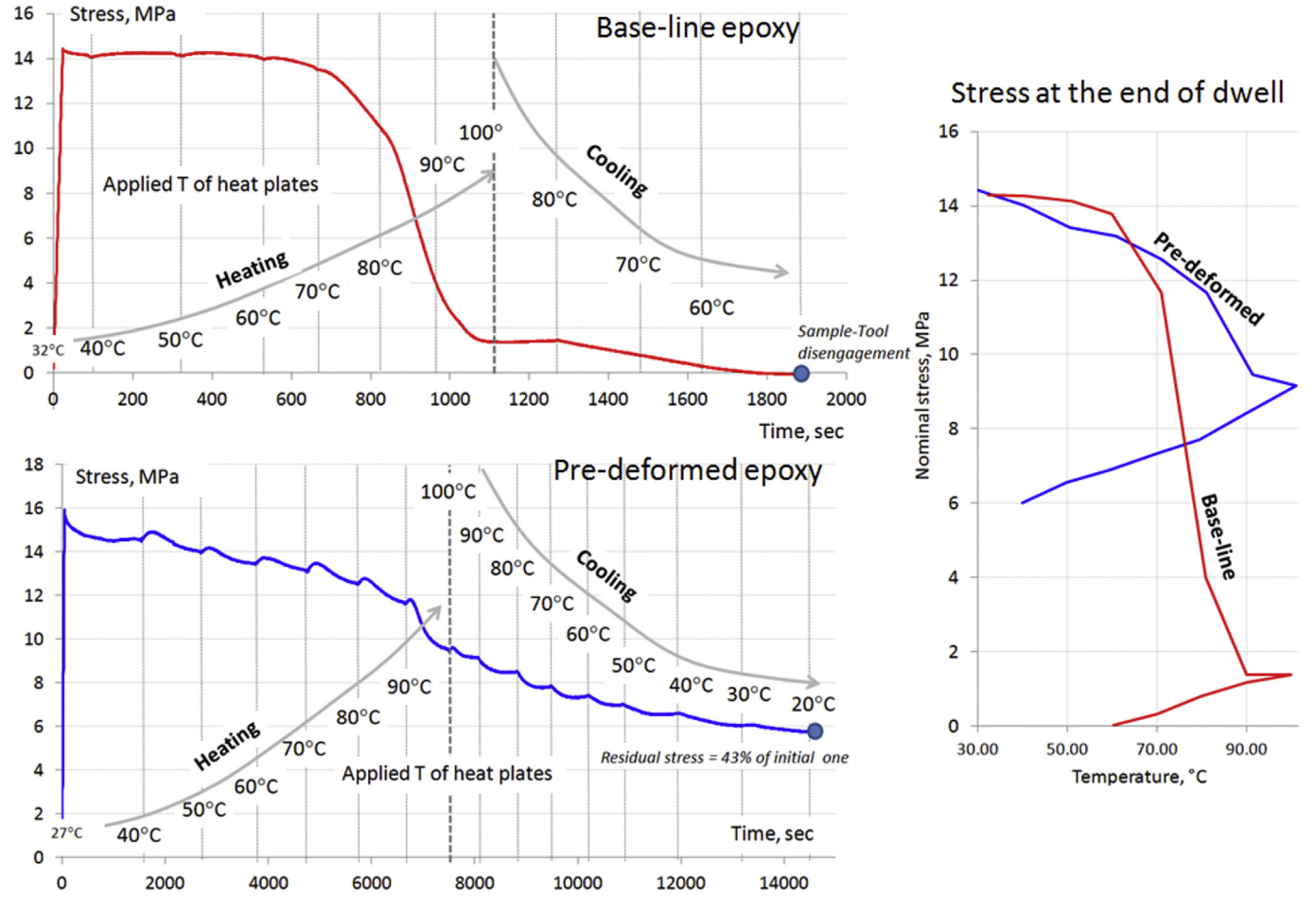

Fig. 7. Stress history of LM pre-deformed and non-deformed (base-line) epoxies under fixed displacement during one thermal cycle (heating to 100 °C and cooling back to room temperature). The temperature values on the right graphs correspond to the temperatures applied to the heating plates. The figure on the right shows stress at the end of dwell temperature interval at the equilibrium of heating, viscous relaxation, and release of accumulated energy in pre-deformed samples.

cycling evidences that the new cross-links were not formed in the process of plastic yielding.

3. The ductility of the pre-deformed samples was reduced. In agreement with observations of polystyrene resin a softening peak soon after the onset of yielding has disappeared after compression (mechanical conditioning) of LM resin. The softening effect, as was suggested by Govaert et al. [10], may be responsible for strain localization and hence have a negative impact leading to early cracking onset.
4. The preliminary results suggest that toughened epoxies demonstrate high yield stresses, which may be beneficial for inter-laminar fracture toughness, compression after impact strength, but have lower strain to failure and hence may face earlier damage onset. However, it is important to emphasize that the large strain to failure observed in shear and compression test does not necessarily translate into the resistance to dilatational component of loading. The ductility in multi-axial straining which takes place in the matrix at the micro scale. The full implications of this behaviour for composite performance invite further study, and we will address this in a future paper.
5. The plastically deformed epoxy samples accumulate energy that can be released upon heating. This was evidenced by both DSC tests and by thermal cycling of loaded samples. In DSC analyses, the samples showed a different signature and an additional exotherm at temperatures below glass transition. The tests on relaxation showed an unusual increase in reaction stress upon heating followed by the relaxation.

7. Conclusions

The high deformation of the resin is not possible in most of the composite applications and hence, the assessment of the physical response of the yielded samples is currently a theoretical question. Yet, understanding of the matrix potential is essential when designing new manufacturing processes, developing new fibre architectures, reinforcements and matrix additives. Based on the conducted testing it becomes clear that if plastic potential of matrices could be at least partly realised (e.g. by reducing contrasts in Poisson's ratios and thermal properties of constituents), it could open a range of possibilities both in terms of mechanical performance of composites and manufacturability of composite structures. If there was a process where fully cured matrix could be deformed without inducing matrix damage, the properties of a composite deformed in this fashion would exhibit a minor decrease of strain to failure but become less sensitive to strain localization and defects due to eliminating softening effects. The yielded resins would retain their stiffness and show potential in terms of releasing the accumulated energy and, hence, improved relaxation behaviour in certain conditions. On the other hand, the response of the toughened resin offers fewer possibilities for mechanical

conditioning or post-cure forming. The test showed that while increasing the yield stress and properties associated with it, the ductility of the composite can be significantly compromised.

The suggested experimental programme highlights several peculiar aspects of resin behaviour and potentially may be used to (a) complement a palette of instruments that can be used for rapid screening of resins for composite applications [23], (b) inform numerical simulation of the resins at molecular scale [24], and (c) modelling of failure and deformation processes at the micro level.

Acknowledgements

The experimental work has been funded by InterCom project CIG PCIG10-GA-2011-304062 (New inter-scale techniques for damage analysis of novel composite architectures) funded by Marie Curie Career Integration Grant of European Commission (FP7). The work was also supported by EPSRC Grant EP/M009149/1: “New generation of manufacturing technologies: liquid print of composite matrices”. The authors express their gratitude to Sam Eggermont and James Artingstall for introductory work and preliminary results, and, within ACCIS, to Dr Julie Etches, Dr Carwyn Ward, and Jusuf Mahadik for help with setting the experimental programme.

References

[1] D.S. Ivanov, S.V. Lomov, F. Baudry, H. Xie, B. Van Den Broucke, I. Verpoest, Failure analysis of triaxial braided composite, Compos. Sci. Technol. 69 (9) (2009) 1372–1380.
[2] S.V. Lomov, D.S. Ivanov, T.C. Truong, I. Verpoest, F. Baudry, K. Vandenbosche, H. Xie, Experimental methodology of study of damage initiation and development in textile composites in tensile test, Compos. Sci. Technol. 68 (12) (2008) 2340–2349.
[3] D.S. Ivanov, S.V. Lomov, A.E. Bogdanovich, M. Karahan, I. Verpoest, Comparative study of tensile properties of non-crimp 3d orthogonal weave and multilayer plain weave e-glass composites. Part 2: comprehensive experimental results, Compos. A 40 (8) (2009) 1144–1157.
[4] E.M. Odom, D.F. Adams, Specimen size effect during tensile testing of an unreinforced polymer, J. Mater. Sci. 27 (7) (1992) 1767–1771.
[5] L. Asp, L. Berglund, A. Gudmundson, Effects of a composite-like stress state on the fracture of epoxies, Comp. Sci. Tech. 53 (1) (1995) 27–37.
[6] Y.M. Liang, K.M. Liechti, On the large deformation and localization behavior of an epoxy resin under multiaxial stress states, Int. J. Solids Struct. 33 (10) (1996) 1479–1500.
[7] W. Chen, F. Lu, M. Cheng, Tension and compression tests of two polymers under quasi-static and dynamic loading, Polym. Test. 21 (2) (2001) 113–121.
[8] B. Fiedler, M. Hojo, S. Ochiai, K. Schulte, M. Ando, Failure behavior of an epoxy matrix under different kinds of static loading, Comp. Sci. Tech. 61 (11) (2001) 1615–1624.
[9] M.Z. Shah Khan, G. Simpson, C.R. Townsend, A comparison of the mechanical properties in compression of two resins, Mater. Lett. 52 (3) (2001) 173–179.
[10] L.E. Govaert, H.G.H. van Melick, H.E.H. Meijer, Temporary toughening of polystyrene through mechanical pre-conditioning, Polymer 42 (3) (2001) 1271–1274.
[11] S. Behzadi, F. Jones, Yielding behavior of model epoxy matrices for fiber reinforced composites: effect of strain rate and temperature, J. Macromol. Sci. Phys. 44 (6) (2005) 993–1005.
[12] J.D. Littell, C.R. Ruggeri, R.K. Goldberg, G.D. Roberts, W.A. Arnold, W.K. Binienda, Measurement of epoxy resin tension, compression, and shear stress- strain curves over a wide range of strain rates using small test specimens, J. Aerosp. Eng. 21 (3) (2008) 162–173.
[13] J.L. Jordan, J.R. Foley, C.R. Siviour, Mechanical properties of Epon 826/DEA epoxy, Mech. Time-Depend Mater. 12 (3) (2008) 249–272.
[14] M.Y. Fard, Y. Liu, A. Chattopadhyay, Characterization of epoxy resin including strain rate effects using digital image correlation system, J. Aerosp. Eng. 25 (2012) 308–319.
[15] J. Chevalier, X.P. Morelle, C. Bailly, P.P. Camanho, T. Pardoen, F. Lani, Micromechanics based pressure dependent failure model for highly cross-linked epoxy resins, Eng. Fract. Mech. 158 (2016) 1–12.
[16] M.Y. Fard, Y. Liu, A. Chattopadhyay, A simplified approach for flexural behavior of epoxy resin materials, J. Strain Anal. 47 (1) (2011) 18–31.
[17] M.Y. Fard, Y. Liu, A. Chattopadhyay, The ratio of flexural strength to uniaxial tensile strength in bulk epoxy resin polymeric materials, Polym. Test. 40 (2014) 156–162.
[18] T. Hobbiebrunken, B. Fiedler, M. Hojo, S. Ochiai, K. Schulte, Microscopic yielding of CF/epoxy composites and the effect on the formation of thermal residual stresses, Comp. Sci. Tech. 65 (10) (2005) 1626–1635.
[19] J. Misumi, R. Ganesh, S. Sockalingam, J.W. Gillespie Jr., Experimental characterization of tensile properties of epoxy resin by using micro-fiber specimens, J Reinf. Plast. Compos. 35 (24) (2016) 1792–1801.
[20] L. Xie, D.W. Cidley, H.A. Hristov, A.F. Yee, Evolution of nanometer voids in polycarbonate under mechanical-stress and thermal-expansion using positron spectroscopy, J. Polym. Sci., Part B Polym. Phys. 33 (1) (1995) 77–84.
[21] M. Aboulfaraj, C. G'sell, D. Mangelinck, G.B. McKenna, Physical aging of epoxy networks after quenching and/or plastic cycling, J. Non-cryst. Solids 172–174 (1994) 615–621.
[22] ASTM, Standard Test Method for Shear Properties of Composite Materials by the V-notched Beam Method, 1993.
[23] K. Tsotsis Th, K.L. Rugg, B.N. Cox, Towards rapid screening of new composite matrix resins, Comp.Sci. Tech. 66 (2006) 1651–1670.
[24] I. Hamerton, W. Tang, J.V. Anguita, S.R.P. Silva, Towards the rational design of polymers using molecular simulation: predicting the effect of cure schedule on thermo-mechanical properties for a cycloaliphatic amine-cured epoxy resin, React. Funct. Polym. 74 (2013) 1–15.